



COMPARATIVE STUDIES OF STANDARD STAINLESS STEEL AND IMPROVISED METALLIC IMPLANTS AND CORROSION INHIBITION POTENTIAL OF *GUAIAECUM OFFICINALE* VIA ELECTROCHEMICAL AND COMPUTATIONAL APPROACHES

*¹Nsidibeabasi Calvin Nwokem, ¹Idowu Elijah Agbele, ¹Uba Sani, ¹Israel Kehinde Omoniyi, ²Gaba Echiobi Emmanuel

¹Department of Chemistry, Ahmadu Bello University, Zaria. Kaduna State, Nigeria
²Department of Veterinary Medicine, Ahmadu Bello University, Zaria. Kaduna State, Nigeria

*Corresponding authors' email: agbeleid2020@gmail.com

ABSTRACT

The malleability and fabrication of metal and associated alloys, as well as their vast range of applications, are significantly influenced by their physicochemical characteristics. Gas chromatograph mass spectrometer revealed the presence of eight (8) bioactive components, which are responsible for the inhibitory activities. Having a maximum inhibition efficiency of 85.17 at an inhibitor dose of 0.5g/L, there is a significantly reduction in reaction number in the presence of *Guaiacum officinale* extract compared to the blank solution. The electrochemical parameters for the improvised metallic biomaterial in 1.0 M HCl solution in the presence and absence of inhibitor concentrations revealed the high polarization region, thus a wide potential range. The addition of the inhibitor affected the anodic and the cathodic partial reactions, which signifies mixed-type mechanism of inhibition. The rate of corrosion mitigation increases in the presence of inhibitors when compared with a blank solution as a result of thin-film formation on metal/solution interface. This work give relevant information on the efficiency of *Guaiacum officinale* as an inhibitor for improvised metallic biomaterial in 1M HCl. The biocompatibility test showed that mechanical and chemical properties are within the recommended values.

Keywords: *Guaiacum officinale*, metallic implants, inhibition

INTRODUCTION

Metal and its alloys have extensive range of utilizations in different industries such as medical, construction, metallurgical among others, due to its physical and chemical features (Ates *et al.* 2020; Vinogradov *et al.* 2019; Yilmaz *et al.* 2020). Metals are characterized by significant changes in their surface properties when exposed to biological, chemical, and biochemical environments, which lead to deterioration of quality as a result of corrosion (Behera *et al.*, 2020; Saha and Kang 2022; Yilmaz *et al.* 2020). Corrosion is a viable and thermodynamic favorable process that causes an adverse effect on metallic material (Amech, 2018). The aggressive media are unavoidably employed in industries, due to manufacture applications that is, oil-well cleaning, industrial acid cleaning, acid pickling, and acid descaling, thus fostered corrosion on metallic substances (Adeniji and Akindehinde 2018; Freer and Powell 2020; Yilmaz *et al.* 2020)

However, researchers have struggled with the negative effects of corrosion on metals over the years. There are corrosion controlling methods such as; paint, plastic, or powder, galvanization, cathodic protection, grease among others. As a result, scientists are seeking corrosion inhibitory methods that are ecofriendly, non-toxic, readily available, applicable at a wide temperature, and cheap. For this reason, a variety of plant materials were employed because of the presence of bioactive components that enhance effective inhibitory activities, cost-effective, and ecofriendly (Dehghani *et al.*, 2019).

Advance still, a quantum mechanical modeling technique called density-functional theory (DFT) is used in chemistry to ascertain the electronic structure of various organic components responsible for corrosion inhibition via computational and theoretical knowledge (Hemmerich and Ecker 2020; Liu 2020; Rodriguez *et al.*, 2020).

Despite the fact that this plant has been the subject of numerous reports, yet no work was done on inhibitory

activities of *Guaiacum officinale* on metal. The objective of this work is to use GC-MS analysis to identify the bioactive ingredients in this plant extract, to investigate their anti-corrosion potential using molecular dynamics simulation, and experimental evaluation of corrosion inhibition efficiency of the extract on a metal surface (Ramezanzadeh *et al.*, 2019).

MATERIALS AND METHODS

Plant collection, preparation and extraction

The exudate of *Guaiacum officinale* are recognized in the field using conventional keys and certified at the herbarium unit of the botany section of Ahmadu Bello University, Zaria, Nigeria. The exudate of *Guaiacum officinale* plant were gathered from the farmyard, pounded and sieved into small particle sizes to increase the surface area before the extraction, extraction was carried out using alcohol, filtered and the filtrate is subjected to the rotatory evaporator at 340K to prevent ethanol contaminants and concentrated the extract.

Mechanical and chemical parameters of the improvised metallic implant and standard stainless steel

Improvised metallic biomaterial implant samples were obtained from solid rods of Fan-guard (makers are ORL and China Mainland) at Zaria, Nigeria. The rods have dimensions of 5mm diameter and were cut into 1cm length for material characterization. The chemical compositions were determined using XRF (model +66 EDX1800B Dand USA) for non-destructive analysis while mechanical properties (such as: tensile stress, tensile strain, young modulus, force and area) were determined using Tensiometer for destructive analysis. The mechanical and chemical properties of metallic implants were determined based on American Standard for Testing and Materials ASTM principles (Bolewski *et al.*, 2020; Egorov *et al.*, 2002; Pandey *et al.*, 2021).

Corrosion studies

Thermometric method

Corrosion tests were carried out in an acidic solution. The beakers containing inhibited and uninhibited HCl media, while the steel samples were immersed. The beakers were sited in a thermostat water bath set at 40°C. Corrosion reaction was monitored and the maximum temperatures of the system containing the test solution and the steel sample are recorded when a steady temperature was obtained. Equations (1) and (2) were employed for the determination of inhibition efficiency from the reaction number values.

$$RN (^{\circ}CMin^{-1}) = \frac{T_2 - T_1}{t} \quad (1)$$

Where T_2 and T_1 are maximum and minimum temperature and time interval (t). The inhibition efficiency (% I) of the inhibitor was calculated based on the reaction number:

$$\%I = \frac{RN_a - RN_p}{RN_a} \quad (2)$$

Where RN_a is the reaction number without inhibitors (blank system) and RN_p is the reaction number containing the inhibitor concentrations and aggressive medium that is 1.0 M HCl solution (Shukla and Ebenso 2011).

Electrochemical measurement

Linear polarization determination were carried out via potentiostat (IVIUM, IVIUM XRE Technologies) and three electrodes comprising platinum using as auxiliary electrode, iron employed as the working electrode, saturated calomel electrode (SCE) as reference at a potential range of $\pm 0.25V$ for stainless steel in HCl medium containing several concentrations of the test inhibitors ranging from 0.1 to 0.5g/L. The scan rate of 0.33 mV/s at 40°C, all measurements was performed in triplicate to encourage reproducible results.

The inhibition efficiencies were calculated using equation 3. and 4 respectively:

$$\%I = \left(1 - \frac{i_{cr}}{i_{in}}\right) \times 100 \quad (3)$$

$$\%I = \frac{R_{ct(in)} - R_{ctr}}{R_{ct(in)}} \times \frac{100}{1} \quad (4)$$

where i_{cr} and i_{in} are the corrosion currents in the absence and presence of the inhibitor respectively and R_{ctr} and $R_{ct(in)}$ are the uninhibited and inhibited charge transfer resistance respectively (Oguzie *et al.* 2014).

Computational consideration

Density functional theory (DFT) is used to calculate molecule and structural properties with excellent precision. Computational simulations of the molecular parameters of different components in the plant extract (A to J) were conducted employing DFT (that is density functional theory) in Spartan 14 programme package. The equilibrium geometry of the selected components in plant extract were carried out at functional hybridization of Becke-3-Lee-Yang-Parr with set of polarization d-functions 6-311G(d) at basis set [B3LYP/6-311G(d)] to achieved full geometry optimization. Computational approach is employed to determine the selectivity of an *N*-electron, mimic the molecular properties and predict the reactivity of the system using quantum chemical methods such as: highest occupied molecular orbital (E_{HOMO}), lowest unoccupied molecular orbital (E_{LUMO}), energy gap (ΔE) difference between ($E_{LUMO} - E_{HOMO}$) energies, ionization energy (I), electron affinity (A), global softness (σ) and global hardness (η) (Awe *et al.* 2015).

RESULTS AND DISCUSSIONS

Table 1: Elemental composition of standard stainless steel and metallic biomaterial employed for the study

S/No	Standard stainless implant	% Elemental Composition A	% Elemental Composition B
1	Fe (93.54)	Fe (98.84)	Fe (98.89)
2	Zn (4.27)	Mn (0.0618)	Ca (0.1203)
3	Zr (<0.28)	Zn (<0.001)	Zn (0.2212)
4	Nb (1.3)	Mg (0.0462)	As (<0.042)
5	Pb (0.22)	C (0.1203)	Kr (<0.008)
6		Si (0.0547)	Nb (0.0553)
7		Al (0.0227)	Mo (0.0361)

Table 2: Mechanical properties of selected metallic biomaterial and standard implants

Samples	Force	UTS	Area	Strain	Young Modulus	% E
A1	966.67	1230.64	0.788	0.188	6532.06	18.84
A2	1450	820.41	1.767	0.896	915.6	89.60
SI	2375	931.37	2.55	0.57	1757.3	57

Comparative studies of improvised metallic implants and standard stainless steels based on mechanical and chemical properties

Table 1 revealed the X-Ray diffraction evaluate, which is a nondestructive process that offers explicit information about the chemical composition, crystallographic structure and physical properties of the material (Pandey *et al.* 2021). Elemental components such as Ni, Co and V are not toxic or they are elements that cannot cause allergic problems, therefore they acceptable and biocompatible. Cobalt offers continuous phase for basic properties as reported by Shen *et al.* (2021). Chromium provides inhibitory effect against metal corrosion via the oxide surface. Molybdenum provides strength and bulk corrosion resistance (Sinnott-Jones, Wharton, and Wood 2005). Nickel and carbon enhance

mechanical properties such as ductility. Therefore, elemental component is a critical in the determination of the biocompatibility of improvised metallic implants as reported by (Jadhav *et al.* 2018).

A mechanically compatible metallic material must offer a favourable combination of low elastic and high mechanical resistance as shown in Table 2. Mechanical properties are physical properties that a material exhibits upon the application of forces. and corroborated by Bartlett *et al.*, (2017). A higher Young's modulus is considered a high priority when designing implants for biomedical applications, especially if the metallic implants have a modulus that is much higher than that of bone (Abraham and Venkatesan 2023; Bagga *et al.* 2016; Renganathan *et al.*, 2021)

Table 3: Thermometric results for the calculation of percent inhibition efficiency and reaction number of *Guaiacum officinale*

C(g/L)	Initial temperature	Max temperature	Reaction number	Percent inhibition
Blank	30	32.6	0.52	-
0.1	30	30.845	0.1690	67.5
0.2	30	30.690	0.1380	73.47
0.3	30	30.482	0.09641	81.46
0.4	30	30.047	0.09069	82.56
0.5	30	30.04	0.07712	85.17

Table 3 clearly revealed that reaction number decreased in the presence of *Guaiacum officinale* extract compared to the blank solution. The inhibition efficiency as expected increased with an increase in the concentration of the inhibitor.

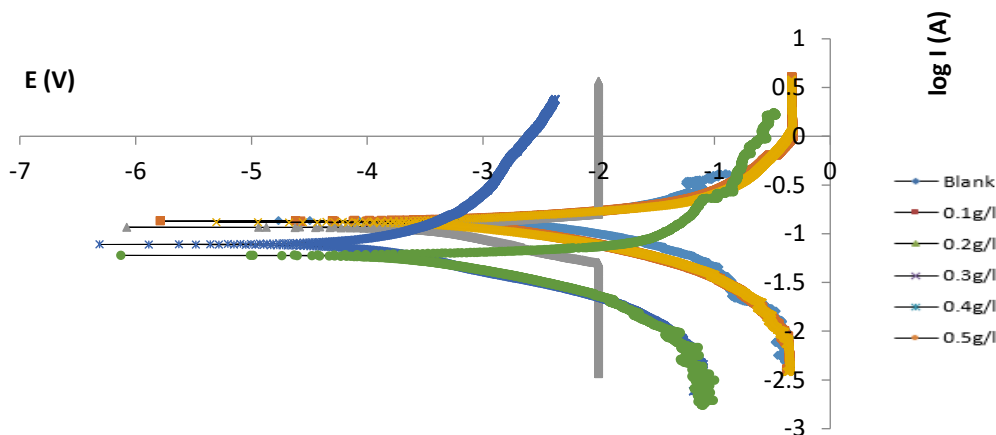


Figure 1: Polarization curve for the corrosion of stainless steel in 1.0 M HCl in the presence and absence of various concentration of *Guaiacum officinale* at 313K

Table 4: Electrochemical parameters and inhibition efficiency values of various inhibitors in the absence and presence of different concentrations of *Terminalia catappa* for the corrosion of improvised biomaterial in 1.0M HCl solution through PDP and LPR methods

Tafel polarization parameters					System	Linear polarization resistance (LPR)	
E_{corr} (Mv)	β_c (mVdec ⁻¹)	β_a (mVdec ⁻¹)	I_{corr} (μ A)	%IE	Concentration	R_p (R/cm ²)	%IE
-851.59	151.2	148.2	1218.0	-	Blank	19.501	-
-856.83	135.5	139.2	596.82	51.91	0.1	59.40	67.17
-941.38	128.6	131.1	377.82	65.98	0.2	75.35	74.12
-1105.8	108.7	125.8	248.47	70.96	0.3	101.15	80.72
-1216.5	101.1	119.6	246.04	79.80	0.4	160.17	87.82
-1412.5	98.5	107.6	183.92	84.90	0.5	256.25	92.39

Potentiodynamic polarization curves for metallic implant in 1M HCl solution in the absence and presence of different inhibitor concentrations at 303K is shown in Figure 1. The electrochemical parameters such as corrosion current density (i_{corr}), corrosion potential (E_{corr}), the cathodic Tafel slope (β_c), anodic Tafel slope (β_a) and inhibition efficiency (IE %) obtained from the potentiodynamic polarization curve is given in Table 4. The polarization resistance values in the presence of the various inhibitor concentrations are determined, resistance was observed to increase in the inhibited solution compared to the blank, indicating that GO inhibited metallic implants against corrosion in the acid medium. Also, the polarization inhibition values in the presence of the various inhibitor concentrations are determined, resistance was observed to increase in the inhibited solution compared to the blank, indicating that GO and TC inhibited metallic implants against corrosion in the acid medium. It can be deduced from the plots that the nature of the polarization curves are the same in both the uninhibited

and inhibited solutions similar to the work of Awe *et al.* (2015), Delfani *et al.* (2021), Lebrini *et al.* 2010 and Umoren *et al.* (2018). However, addition of both *Guaiacum officinale* as inhibitor to the acidic medium reduced the corrosion rate of the metallic implant as evidenced in the shifting of the corrosion current density to regions of lower values in comparison to the blank system, indicating the corrosion inhibiting ability of the plant exudates (Etteyeb and NÓvoa, 2016). This revealed that the corrosion potential (E_{corr}) in the presence of TC shifted to noble values relative to the blank, suggesting that the GC are mixed-type inhibitors (Bentrah, Rahali, and Chala 2014). Both anodic and cathodic current densities are reduced as concentration of inhibitors increased; this is due to the effect of the coating by the active inhibitory compounds of the plant extract on the metal surface (Abdullah *et al.* 2019; Awe *et al.* 2015).

It has been reported that the inhibitory corrosion potential of a molecule is a function of electronic properties which can be

inferred from its quantum chemical parameters (Xavier *et al.*, 2015) such as energy gap ($\Delta E = E_{LUMO} - E_{HOMO}$), electronegativity, polarization surface area, global hardness and global softness. These parameters are reported in Table 1. The energy gap is a vital parameter for determining stability of a system. The wider the energy gap, the more stable a molecule is, hence, the less its reactivity. It is the difference between the energies of highest occupied molecular orbital (E_{HOMO}) and the lowest unoccupied molecular orbitals (E_{LUMO}) (Obot, Obi-Egbedi, and Eseola 2011). The ability of an inhibitor to donate electrons into the low-lying vacant orbitals of a metal is a function of its ionization potential (I) which is related to the energy of highest occupied molecular orbital, E_{HOMO} , by the expression: $I = -E_{HOMO}$. Also, the electron affinity (A) of an inhibitor is related to the energy of lowest unoccupied molecular orbital (E_{LUMO}), that is $A = -E_{LUMO}$, which indicates the tendency of the inhibitor to accept electrons. As the energy gap (ΔE) of inhibitors decreases, there is a corresponding increase in their reactivity, hence, an increase in the predictive corrosion inhibition potential. This band gap is related to I and A by the expression: $\Delta E = I - A$. The energy gap elucidates the ultimate charge transfer interaction inside the molecule; and it is useful in evaluating molecular electrical properties. According to the frontier molecular orbital theory (FMO), the energy gap ($\Delta E = E_{LUMO} - E_{HOMO}$) is related to the inhibition efficiency of inhibitor molecule. It has been reported that low values of ΔE will provide good inhibition efficiency, because the energy for removing an electron from the last occupied orbital will be low (Ameh 2015; Arukalam 2014). For instance, compounds that have a high energy gap are stable, and hence are chemically harder than compounds having a small energy gap (Leila *et al.*, 2018; Madkour *et al.*, 2018; Ruiz-Morales and Mullins, 2009). The shapes and symmetries of the organic compounds are employed in predicting the corrosion inhibition reaction, the reactivity of the organic compound and predicting the chemical reaction product (Eddy *et al.*, 2011). Both molecular and structural properties have great correlation with corrosion inhibition efficiency (Khaled,

Babić-Samardžija, and Hackerman 2005). The dipole moment (μ) parameter is a vital parameter which is connected with the molecular stability in polar environments. In this research, the experimental dipole moment is not identified. The calculated dipole moments in gaseous phase are shown in Table 5. The influences of the polar environment (i.e. acetone, toluene, ethanol among others) are not considered in comparison the dipole moment values but carried out only in gas phase. Among the considered compounds 1,2 -benzothiazol-3-amine has the highest dipole moment in the gas phase among the selected aromatic based compounds in the plant exudates, because it has a higher dipole interaction, therefore, it indicates strong dipole-dipole interaction between the inhibitor molecule and the iron surface.

It is noticed that some dipole moments determined in the selected organic compounds in the plant exudates were higher than the dipole moment of water that is 1.88 Debye (Li *et al.*, 2022). This implies that some of the organic compounds in the plant exudates will displace the water molecules from the metal surface, get chemically adsorbed onto the metal surface thereby inhibit in metallic implants surface against corrosion (Ameh, 2015; Dehdab *et al.*, 2016). In this work, higher dipole moment values were observed in the compounds possessing in electron donor (i.e. N, O, Cl, S) compared to those with electron- acceptor groups (i.e. H, C, H) in the studied gas phase (Aigbogun and Adebayo, 2021; Miar *et al.*, 2021). The global electrophilicity index (ω), introduced by (Parr *et al.*, 1999) is based on thermodynamic properties and measures the favorable change in energy when a chemical system or compound attains saturation by the addition of electrons. It can be defined as the decrease in energy due to the flow of electrons from the donor (E_{HOMO}) to the acceptor (E_{LUMO}) in molecules. It also plays an important role in determining the chemical reactivity of a system. Compounds having greater values of chemical potential are more reactive than those with small electronic chemical potentials (Ayers *et al.*, 2006).

Table 5: DFT at B3LYP/6-311G(d) at level theory to validate quantum chemical calculations of plant extract components

Compounds	E_{HOMO} eV	E_{LUMO} eV	DM debye	MW (amu)	MA (\AA^2)	MV (\AA^3)	PSA (\AA^2)	Pol	Ovality	Log P
C ₁₆ H ₁₂ O ₅	-9.18	-0.93	5.22	284.27	289.61	274.97	62.32	61.73	1.42	1.66
C ₂₃ H ₄₆	-9.17	1.5	0.58	322.62	489.54	434.29	0	74.09	1.77	9.54
C ₁₆ H ₃₀ O ₂	-10.8	0.57	5.03	254.41	346.3	308.07	34.48	63.69	1.57	5.19
C ₁₆ H ₃₄ O	-9.46	0.54	1.83	282.46	397.41	351.46	34.78	67.53	1.65	6.29
C ₁₈ H ₃₄ O ₂	-9.59	2.3	1.62	242.45	357.83	318.05	6.74	64.38	1.59	5.8
C ₁₄ H ₁₁ C ₁₂ N O ₂	-8.67	-0.61	4.25	296.15	278.83	266.57	42.83	61.1	1.39	3.6
C ₂₂ H ₄₄ O ₂	-1.73	0.5	2.38	340.59	489.31	430.66	34.87	73.67	1.77	8.28
C ₂₀ H ₃₄ O ₂	-9.5	0.51	1.57	306.49	413.82	378.58	33.43	69.73	1.64	6.48

CONCLUSION

Corrosion inhibition of improvised metallic implants using *Guaiacum officinale* in 1M HCl solution was measured by thermometric and electrochemical methods at different temperatures. The result showed that corrosion rate was considerably declined in presence of the *Guaiacum officinale* extract and inhibition efficiency increased with increasing the concentration of extract. 85.17% inhibition efficiency was found in 1M HCl at 0.5g/L inhibitor concentration of plant extract. The condition of mixed inhibitor adsorption on the implant surface was displayed by potentiodynamic

polarization. Computational investigations revealed a remarkable report that supported by experimental results. All the theoretical parameters ensure that *Guaiacum officinale* extract can act as an effectual blanket layer and minimise the corrosion process.

REFERENCES

Abdullah, Nurul Hidayah, Kamyar Shameli, Ezzat Chan Abdullah, and Luqman Chuah Abdullah. 2019. "Solid Matrices for Fabrication of Magnetic Iron Oxide Nanocomposites: Synthesis, Properties, and Application for

- the Adsorption of Heavy Metal Ions and Dyes." *Composites Part B: Engineering* 162:538–68.
- Abraham, Adarsh Mathew, and Subramani Venkatesan. 2023. "A Review on Application of Biomaterials for Medical and Dental Implants." *Proceedings of the Institution of Mechanical Engineers, Part L: Journal of Materials: Design and Applications* 237(2):249–73.
- Adeniji, Shola Elijah, and Bamigbola Abiola Akindehinde. 2018. "Comparative Analysis of Adsorption and Corrosion Inhibitive Properties of Ethanol Extract of Dialium Guineense Leaves for Mild Steel in 0.5 M HCl." *Journal of Electrochemical Science and Engineering* 8(3):219–26.
- Aigbogun, Jane A., and Matthew A. Adebayo. 2021. "Green Inhibitor from *Thaumatococcus Daniellii* Benn for Corrosion Mitigation of Mild Steel in 1M HCl." *Current Research in Green and Sustainable Chemistry* 4:100201.
- Ameh, Paul Ocheje. 2015. "A Comparative Study of the Inhibitory Effect of Gum Exudates from *Khaya Senegalensis* and *Albizia Ferruginea* on the Corrosion of Mild Steel in Hydrochloric Acid Medium." *International Journal of Metals* 2015.
- Arukalam, I. O. 2014. "Durability and Synergistic Effects of KI on the Acid Corrosion Inhibition of Mild Steel by Hydroxypropyl Methylcellulose." *Carbohydrate Polymers* 112:291–99.
- Ates, Burhan, Suleyman Koytepe, Ahmet Ulu, Canbolat Gurses, and Vijay Kumar Thakur. 2020. "Chemistry, Structures, and Advanced Applications of Nanocomposites from Biorenewable Resources." *Chemical Reviews* 120(17):9304–62.
- Awe, F. E., S. O. Idris, M. Abdulwahab, and E. E. Oguzie. 2015. "Theoretical and Experimental Inhibitive Properties of Mild Steel in HCl by Ethanolic Extract of *Boscia Senegalensis*." *Cogent Chemistry* 1(1):1112676.
- Ayers, Paul W., Robert G. Parr, and Ralph G. Pearson. 2006. "Elucidating the Hard/Soft Acid/Base Principle: A Perspective Based on Half-Reactions." *The Journal of Chemical Physics* 124(19):194107.
- Bagga, Manpreet Kaur, Ranu Gadi, Ompal Singh Yadav, Raman Kumar, Rashi Chopra, and Gurmeet Singh. 2016. "Investigation of Phytochemical Components and Corrosion Inhibition Property of *Ficus Racemosa* Stem Extract on Mild Steel in H₂SO₄ Medium." *Journal of Environmental Chemical Engineering* 4(4):4699–4707.
- Bartlett, Michael D., Navid Kazem, Matthew J. Powell-Palm, Xiaonan Huang, Wenhuan Sun, Jonathan A. Malen, and Carmel Majidi. 2017. "High Thermal Conductivity in Soft Elastomers with Elongated Liquid Metal Inclusions." *Proceedings of the National Academy of Sciences* 114(9):2143–48.
- Behera, Ajit, P. Mallick, and S. S. Mohapatra. 2020. "Nanocoatings for Anticorrosion." *Corrosion Protection at the Nanoscale* 227–43. doi: 10.1016/b978-0-12-819359-4.00013-1.
- Bentrah, Hamza, Youssef Rahali, and Abdelouahad Chala. 2014. "Gum Arabic as an Eco-Friendly Inhibitor for API 5L X42 Pipeline Steel in HCl Medium." *Corrosion Science* 82:426–31.
- Bolewski, Andrzej, Marta Matosz, Władysław Pohorecki, and Julio M. del Hoyo-Meléndez. 2020. "Comparison of Neutron Activation Analysis (NAA) and Energy Dispersive X-Ray Fluorescence (XRF) Spectrometry for the Non-Destructive Analysis of Coins Minted under the Early Piast Dynasty." *Radiation Physics and Chemistry* 171:108699.
- Dehdab, Maryam, Mehdi Shahraki, and Sayyed Mostafa Habibi-Khorassani. 2016. "Theoretical Study of Inhibition Efficiencies of Some Amino Acids on Corrosion of Carbon Steel in Acidic Media: Green Corrosion Inhibitors." *Amino Acids* 48(1):291–306.
- Dehghani, Ali, Ghasem Bahlakeh, Bahram Ramezanzadeh, and Mohammad Ramezanzadeh. 2019. "Potential of Borage Flower Aqueous Extract as an Environmentally Sustainable Corrosion Inhibitor for Acid Corrosion of Mild Steel: Electrochemical and Theoretical Studies." *Journal of Molecular Liquids* 277:895–911.
- Delfani, Fatemeh, Nader Rahbar, Cyrus Aghanajafi, Ali Heydari, and Abdollah KhalesiDoost. 2021. "Utilization of Thermoelectric Technology in Converting Waste Heat into Electrical Power Required by an Impressed Current Cathodic Protection System." *Applied Energy* 302:117561.
- Eddy, Nnabuk O., Femi E. Awe, Casmir E. Gimba, Nkechi O. Ibis, and Eno E. Ebenso. 2011. "QSAR, Experimental and Computational Chemistry Simulation Studies on the Inhibition Potentials of Some Amino Acids for the Corrosion of Mild Steel in 0.1 M HCl." *Int. J. Electrochem. Sci* 6(4):931–57.
- Egorov, Viacheslav I., Ilia V Schastliltsev, Edward V Prut, Andrey O. Baranov, and Robert A. Turusov. 2002. "Mechanical Properties of the Human Gastrointestinal Tract \$." 35:1417–25.
- Etteyeb, N., and X. R. Nóvoa. 2016. "Inhibition Effect of Some Trees Cultivated in Arid Regions against the Corrosion of Steel Reinforcement in Alkaline Chloride Solution." *Corrosion Science* 112:471–82.
- Freer, Robert, and Anthony V. Powell. 2020. "Realising the Potential of Thermoelectric Technology: A Roadmap." *Journal of Materials Chemistry C* 8(2):441–63. doi: 10.1039/c9tc05710b.
- Hemmerich, Jennifer, and Gerhard F. Ecker. 2020. "In Silico Toxicology: From Structure--Activity Relationships towards Deep Learning and Adverse Outcome Pathways." *Wiley Interdisciplinary Reviews: Computational Molecular Science* 10(4):e1475.
- Jadhav, Kiran, H. R. Rajeshwari, Swapnil Deshpande, Satveer Jagwani, Dinesh Dhamecha, Sunil Jalalpure, Karthikeyan Subburayan, and Dwarkadas Baheti. 2018. "Phytosynthesis of Gold Nanoparticles: Characterization, Biocompatibility, and Evaluation of Its Osteoinductive Potential for Application in Implant Dentistry." *Materials Science and Engineering: C* 93:664–70.
- Khaled, K. F., K. Babić-Samardžija, and N. Hackerman.

2005. "Theoretical Study of the Structural Effects of Polymethylene Amines on Corrosion Inhibition of Iron in Acid Solutions." *Electrochimica Acta* 50(12):2515–20.
- Lebrini, M., Florent Robert, and C. Roos. 2010. "Inhibition Effect of Alkaloids Extract from *Annona Squamosa* Plant on the Corrosion of C38 Steel in Normal Hydrochloric Acid Medium." *International Journal of Electrochemical Science* 5(11):1698–1712.
- Leila, Bouzidi, Haffar Djahida, Abdi Djamila, Mouzali Saida, and Chafaa Salah. 2018. "Inhibitive Properties and Quantum Chemical Calculations of a New Synthesized Schiff Base 1-[(3-hydroxyphenylamino) Methylene]-Naphthalen-2-One for XC48 in Hydrochloric Acid Solution." *Int. J. Electrochem. Sci* 13:6734–55.
- Li, Songqi, Yuetian Liu, Liang Xue, and Dongdong Zhu. 2022. "Theoretical Insight into the Effect of Polar Organic Molecules on Heptane-Water Interfacial Properties Using Molecular Dynamic Simulation." *Journal of Petroleum Science and Engineering* 212:110259.
- Liu, Zi-Kui. 2020. "Computational Thermodynamics and Its Applications." *Acta Materialia* 200:745–92.
- Madkour, Loutfy H., Sava Kaya, Lei Guo, and Cemal Kaya. 2018. "Quantum Chemical Calculations, Molecular Dynamic (MD) Simulations and Experimental Studies of Using Some Azo Dyes as Corrosion Inhibitors for Iron. Part 2: Bis-Azo Dye Derivatives." *Journal of Molecular Structure* 1163:397–417.
- Miar, Marzieh, Abolfazl Shiroudi, Khalil Pourshamsian, Ahmad Reza Oliay, and Farhad Hatamjafari. 2021. "Theoretical Investigations on the HOMO-LUMO Gap and Global Reactivity Descriptor Studies, Natural Bond Orbital, and Nucleus-Independent Chemical Shifts Analyses of 3-Phenylbenzo [d] Thiazole-2 (3 H)-Imine and Its Para-Substituted Derivatives: Solvent And." *Journal of Chemical Research* 45(1–2):147–58.
- Obot, I. B., N. O. Obi-Egbedi, and A. O. Eseola. 2011. "Anticorrosion Potential of 2-Mesityl-1H-Imidazo [4, 5-f][1, 10] Phenanthroline on Mild Steel in Sulfuric Acid Solution: Experimental and Theoretical Study." *Industrial & Engineering Chemistry Research* 50(4):2098–2110.
- Oguzie, E. E., M. A. Chidiebere, K. L. Oguzie, C. B. Adindu, and H. Momoh-Yahaya. 2014. "Biomass Extracts for Materials Protection: Corrosion Inhibition of Mild Steel in Acidic Media by Terminalia Chebula Extracts." *Chemical Engineering Communications* 201(6):790–803.
- Pandey, Akhilesh, Sandeep Dalal, Shankar Dutta, and Ambesh Dixit. 2021. "Structural Characterization of Polycrystalline Thin Films by X-Ray Diffraction Techniques." *Journal of Materials Science: Materials in Electronics* 32(2):1341–68.
- Parr, Robert G., László v Szentpály, and Shubin Liu. 1999. "Electrophilicity Index." *Journal of the American Chemical Society* 121(9):1922–24.
- Ramezanzadeh, Mohammad, Ghasem Bahlakeh, Zahra Sanaei, and Bahram Ramezanzadeh. 2019. "Corrosion Inhibition of Mild Steel in 1 M HCl Solution by Ethanolic Extract of Eco-Friendly *Mangifera Indica* (Mango) Leaves: Electrochemical, Molecular Dynamics, Monte Carlo and Ab Initio Study." *Applied Surface Science* 463:1058–77.
- Renganathan, Gunarajulu, Narasimhaswamy Tanneru, and Suguna Lakshmi Madurai. n.d. *10. Orthopedical and Biomedical Applications of Titanium and Zirconium Metals*. Elsevier Ltd.
- Rodríguez, José A., Julián Cruz-Borbolla, Pablo A. Arizpe-Carreón, and Evelin Gutiérrez. 2020. "Mathematical Models Generated for the Prediction of Corrosion Inhibition Using Different Theoretical Chemistry Simulations." *Materials* 13(24):5656.
- Ruiz-Morales, Yosadara, and Oliver C. Mullins. 2009. "Measured and Simulated Electronic Absorption and Emission Spectra of Asphaltenes." *Energy & Fuels* 23(3):1169–77.
- Saha, Sourav Kr, and Namhyun Kang. 2022. "Corrosion: Basics, Economic Adverse Effects, and Its Mitigation." *Carbon Allotropes: Nanostructured Anti-Corrosive Materials* 67.
- Shen, Yabin, Hongjin Xue, Shaohua Wang, Zhaomin Wang, Dongyu Zhang, Dongming Yin, Limin Wang, and Yong Cheng. 2021. "A Highly Promising High-Nickel Low-Cobalt Lithium Layered Oxide Cathode Material for High-Performance Lithium-Ion Batteries." *Journal of Colloid and Interface Science* 597:334–44.
- Shukla, Sudhish K., and Eno E. Ebenso. 2011. "Corrosion Inhibition, Adsorption Behavior and Thermodynamic Properties of Streptomycin on Mild Steel in Hydrochloric Acid Medium." *Int. J. Electrochem. Sci* 6(8):3277–91.
- Sinnett-Jones, P. E., J. A. Wharton, and R. J. K. Wood. 2005. "Micro-Abrasion-Corrosion of a CoCrMo Alloy in Simulated Artificial Hip Joint Environments." *Wear* 259(7–12):898–909.
- Umoren, Saviour A., Moses M. Solomon, Ime B. Obot, and Rami K. Sulciman. 2018. "Comparative Studies on the Corrosion Inhibition Efficacy of Ethanolic Extracts of Date Palm Leaves and Seeds on Carbon Steel Corrosion in 15% HCl Solution." *Journal of Adhesion Science and Technology* 32(17):1934–51.
- Vinogradov, Alexei, Evgeni Vasilev, Vladimir I. Kopylov, Mikhail Linderov, Alexander Brilevesky, and Dmitry Merson. 2019. "High Performance Fine-Grained Biodegradable Mg-Zn-Ca Alloys Processed by Severe Plastic Deformation." *Metals* 9(2):186.
- Yilmaz, Bengi, Ahmet Engin Pazarceviren, Aysen Tezcaner, and Zafer Evis. 2020. "Historical Development of Simulated Body Fluids Used in Biomedical Applications: A Review." *Microchemical Journal* 155(February):104713. doi: 10.1016/j.microc.2020.104713.

